

# Influence of magnetic field on optical response in a degenerate four-level lambda-type atomic system

Nguyen Thuy Tram<sup>1</sup>, Nguyen Thi Phuong Anh<sup>1</sup>, Nguyen Thi Ngoc<sup>1</sup>, Hoang Thi Ngoc Yen<sup>1</sup>, Cao Thi Thao<sup>1</sup>, Luong Thi Yen Nga<sup>1</sup>, Ho Hai Quang<sup>1</sup>, Nguyen Thi Kieu Oanh<sup>2</sup> and Le Van Doai<sup>1,†</sup>

<sup>1</sup>Vinh University, 182 Le Duan Street, Nghe An Province, Vietnam

<sup>2</sup>Nguyen Trai High School, Hac Thanh Ward, Thanh Hoa Province, Vietnam

E-mail: <sup>†</sup>doailv@vinhuni.edu.vn

Received 19 September 2025

Accepted for publication 5 December 2025

Published 5 March 2026

**Abstract.** *We theoretically investigate the optical response of a degenerate four-level  $\Lambda$ -type atomic system under the influence of an external magnetic field. The applied magnetic field lifts the degeneracy of the ground sublevels via the Zeeman effect, thereby altering the two-photon resonance conditions for electromagnetically induced transparency (EIT) formation and causing the atomic response to evolve from single-EIT to double-EIT, accompanied by shifts in the EIT positions. Such variations in the EIT positions result in corresponding changes in the dispersion and group index curves, allowing the selection of desired frequency regions for different response regimes. As a result, the system can switch between transparency and absorption, as well as between slow and fast light. These findings highlight the feasibility of controlling light propagation via magnetic field, with potential applications in optical switching and quantum information technologies.*

Keywords: effects of atomic coherence; electromagnetically induced transparency (EIT); optical response.

Classification numbers: 42.50.Nn; 42.50.Gy; 42.65.-k.

## 1. Introduction

Controlling the fundamental optical properties of an atomic medium, such as absorption, dispersion, and group index, plays a crucial role in modern quantum and nonlinear optics. The ability to control absorption, dispersion and the group velocity of light pulses enables the realization of advanced photonic functionalities, including slow and fast light propagation, high-efficiency optical switching, and enhanced nonlinear interactions. In particular, the group index, governed by the slope of the dispersion profile, determines whether a medium supports slow or

fast light and is therefore essential for applications in optical communication, information storage, and quantum information processing.

Electromagnetically induced transparency (EIT) provides a well-established mechanism to manipulate these optical properties. Originating from quantum interference between atomic transition pathways, EIT enables the elimination of resonant absorption and the emergence of steep dispersion in an otherwise opaque medium [1, 2]. Simple EIT configurations are usually realized in three-level systems of  $\Lambda$ -,  $V$ -, or ladder-type configurations with single EIT [3]. Subsequently, studies have been extended to multi-level atomic systems exhibiting multiple EIT windows [4]. EIT-based media have found applications in diverse areas, including slow and fast light [5, 6], enhanced Kerr nonlinearity [7, 8], optical switching and bistability [9–11], coherent pulse propagation [12, 13] and so on. These studies have demonstrated that the optical properties of atomic systems can be effectively manipulated by tuning the parameters of the applied laser fields.

In addition to optical fields, an external magnetic field has emerged as an effective tool for manipulating atomic coherence. The magnetic field modifies the atomic energy levels through the Zeeman effect, thereby altering absorption, dispersion, and group index [14–17]. This approach has been used to control light propagation [18–20], enhance Kerr nonlinearity [21–23], and realize tunable optical switching and bistability [24, 25]. Although previous studies [19, 20] have examined the influence of a magnetic field on the group index of light, they were conducted in a single-EIT configuration with only one control field. The presence of an external magnetic field induces Zeeman splitting of multiple sublevels, which can readily be extended to multi-control-field configurations capable of producing responses in multiple EIT windows.

In this work, we focus on a degenerate four-level  $\Lambda$ -type atomic system where an external magnetic field is applied to remove the degeneracy among the sublevels. By constructing an analytical model and solving the density matrix equations under steady-state conditions, we investigate how the magnetic field influences the absorption, dispersion, and group index of the system. Our results reveal that the magnetic field can induce a transition from a single-EIT to a double-EIT regime, allowing straightforward manipulation of absorption, dispersion and light propagation characteristics. Specifically, we show that the dispersion can switch between normal and anomalous regimes and so the group index can be tuned between positive (slow light) and negative (fast light) values. These findings highlight the magnetic field as a powerful knob for controlling optical responses in multilevel atomic systems, with potential applications in slow/fast light technology, optical switching, and quantum information processing.

## 2. Theoretical model

The schematic configuration of the quantum system under investigation is shown in Fig. 1. The system is placed in an external magnetic field to remove the degeneracy of the Zeeman sublevels, like the approach used in Ref. [20]. By applying three laser fields with appropriate polarizations (as indicated in Fig. 1), the model can be arranged to form a four-level  $\Lambda$ -type configuration. Specifically, a weak probe laser field  $E_p$  with right-circularly polarized component  $\sigma^+$  (carrier frequency  $\omega_p$  and Rabi frequency  $\Omega_p$ ) and a signal laser field  $E_s$  with left-circularly polarized component  $\sigma^-$  (carrier frequency  $\omega_s$  and Rabi frequency  $\Omega_s$ ) are applied to the transitions  $|1\rangle\leftrightarrow|4\rangle$  (transition frequency  $\omega_{41}$ ) and  $|2\rangle\leftrightarrow|4\rangle$  (transition frequency  $\omega_{42}$ ), respectively. The transition  $|3\rangle\leftrightarrow|4\rangle$  of frequency  $\omega_{43}$  is driven by a control laser field  $E_c$  with linearly polarized component  $\pi$

(carrier frequency  $\omega_c$  and Rabi frequency  $\Omega_c$ ). Levels  $|1\rangle$ ,  $|2\rangle$  and  $|4\rangle$  are in a three-level lambda-type configuration and levels  $|1\rangle$ ,  $|3\rangle$  and  $|4\rangle$  form another three-level lambda-type configuration. Consequently, this system is equivalent to the combination of two usual lambda-type subsystems coupled by a common probe field  $E_p$ . The Zeeman shift between the level  $m_F = 0$  and the level  $m_F = \pm 1$  of the ground state is given by  $\hbar\Delta_B = \mu_B m_F g_F B$  with  $\mu_B$  is the Bohr magneton,  $g_F$  is the Landé factor, and  $m_F = \pm 1$  is the magnetic quantum number of the corresponding Zeeman sublevels. All electrons are assumed to be initially optically pumped into the states  $|1\rangle$  and  $|2\rangle$ , which are therefore taken to have equal incoherent populations, i.e.,  $\rho_{11} = \rho_{22} \approx \frac{1}{2}$ . It should be noted that the model in Ref. [20] uses a probe laser field with two components of left- and right-circular polarization, together with a single control laser field, forming a three-level cascade-type configuration for each circularly polarized component of the probe field.

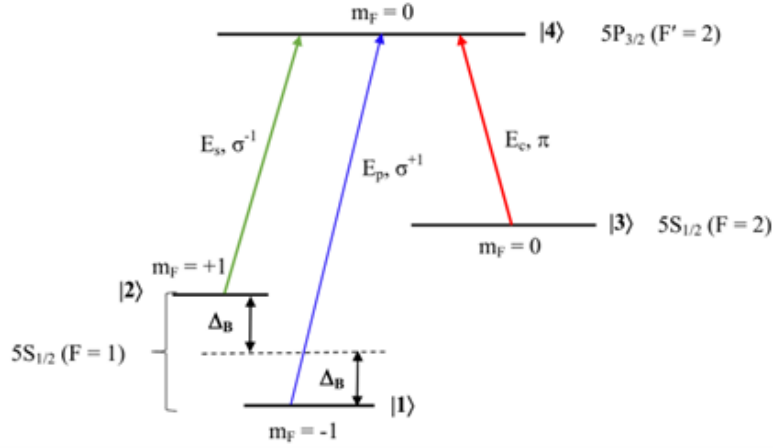


**Fig. 1.** The schematic configuration of a degenerate four-level  $\Lambda$ -type atomic system under an external magnetic field. The specific states are chosen for the  $^{87}\text{Rb}$  atom.

Under the rotating-wave and the electric-dipole approximations, the total Hamiltonian in the interaction picture can be expressed as

$$H = \hbar \begin{bmatrix} 0 & 0 & 0 & \frac{1}{2}\Omega_p \\ 0 & (\Delta_p + \Delta_B) - (\Delta_s - \Delta_B) & 0 & \frac{1}{2}\Omega_s \\ 0 & 0 & (\Delta_p + \Delta_B) - \Delta_c & \frac{1}{2}\Omega_c \\ \frac{1}{2}\Omega_p & \frac{1}{2}\Omega_s & \frac{1}{2}\Omega_c & (\Delta_p + \Delta_B) \end{bmatrix} \quad (1)$$

where  $\Delta_p = \omega_p - \omega_{41}$ ,  $\Delta_s = \omega_s - \omega_{42}$  and  $\Delta_c = \omega_c - \omega_{43}$  are the frequency detunings of the probe, signal, and control fields from the corresponding atomic transitions.  $\Delta_B$  is the Zeeman shift of levels  $|1\rangle$  and  $|2\rangle$  in the presence of the magnetic field and  $\Delta_B$  is taken to zero for zero magnetic field.  $\Omega_p = \frac{d_{41}E_p}{2\hbar}$ ,  $\Omega_s = \frac{d_{42}E_s}{2\hbar}$ , and  $\Omega_c = \frac{d_{43}E_c}{2\hbar}$  with  $d_{mn}$  being the electric-dipole matrix element associated with the transition from the level  $|m\rangle$  to the level  $|n\rangle$ . In the above derivation process of Hamiltonian (1), we have taken the ground state  $|1\rangle$  as the energy origin for the sake of simplicity. The population decay rates from the excited state  $|4\rangle$  to the ground states  $|1\rangle$ ,  $|2\rangle$ , and  $|3\rangle$  are  $\Gamma_{41}$ ,  $\Gamma_{42}$  and  $\Gamma_{43}$ , respectively. Meanwhile, the relaxation rates of atomic coherence between the ground

levels  $|1\rangle$ ,  $|2\rangle$ , and  $|3\rangle$  are negligible because the corresponding transitions are non-electric-dipole allowed.

The dynamical evolution of atomic-field systems is governed by the following optical Bloch equation for the density matrix as

$$\dot{\rho} = -\frac{i}{\hbar}[H, \rho] + \Lambda\rho, \quad (2)$$

where  $\Lambda\rho$  represents the relaxation processes.

In combination with the Hamiltonian  $H$ , we obtain the equations of motion for the density matrix elements as follows:

$$\dot{\rho}_{11} = \Gamma_{41}\rho_{44} + \frac{i}{2}\Omega_p(\rho_{14} - \rho_{41}), \quad (3)$$

$$\dot{\rho}_{22} = \Gamma_{44}\rho_{44} + \frac{i}{2}\Omega_s(\rho_{24} - \rho_{42}), \quad (4)$$

$$\dot{\rho}_{33} = \Gamma_{43}\rho_{44} + \frac{i}{2}\Omega_c(\rho_{34} - \rho_{43}), \quad (5)$$

$$\dot{\rho}_{44} = -(\Gamma_{41} + \Gamma_{42} + \Gamma_{43})\rho_{44} + \frac{i}{2}\Omega_p(\rho_{41} - \rho_{14}) + \frac{i}{2}\Omega_s(\rho_{42} - \rho_{24}) + \frac{i}{2}\Omega_c(\rho_{43} - \rho_{34}), \quad (6)$$

$$\dot{\rho}_{21} = i[(\Delta_p + \Delta_B) - (\Delta_s - \Delta_B)]\rho_{21} + \frac{i}{2}\Omega_p\rho_{24} - \frac{i}{2}\Omega_s\rho_{41}, \quad (7)$$

$$\rho_{31} = i[(\Delta_p + \Delta_B) - \Delta_c]\rho_{31} + \frac{i}{2}\Omega_p\rho_{34} - \frac{i}{2}\Omega_c\rho_{41}, \quad (8)$$

$$\dot{\rho}_{41} = [i(\Delta_p + \Delta_B) - \gamma_{41}]\rho_{41} + \frac{i}{2}\Omega_p(\rho_{44} - \rho_{11}) - \frac{i}{2}\Omega_s\rho_{21} - \frac{i}{2}\Omega_c\rho_{31}, \quad (9)$$

$$\dot{\rho}_{32} = i[(\Delta_s - \Delta_B) - \Delta_c]\rho_{32} + \frac{i}{2}\Omega_s\rho_{34} - \frac{i}{2}\Omega_c\rho_{42}, \quad (10)$$

$$\dot{\rho}_{42} = [i(\Delta_s - \Delta_B) - \gamma_{42}]\rho_{42} + \frac{i}{2}\Omega_s(\rho_{44} - \rho_{22}) - \frac{i}{2}\Omega_p\rho_{12} - \frac{i}{2}\Omega_c\rho_{32}, \quad (11)$$

$$\dot{\rho}_{43} = (i\Delta_c - \gamma_{43})\rho_{43} + \frac{i}{2}\Omega_c(\rho_{44} - \rho_{33}) - \frac{i}{2}\Omega_p\rho_{13} - \frac{i}{2}\Omega_s\rho_{23}, \quad (12)$$

together with  $\rho_{ij} = \rho_{ji}^*$  and  $\rho_{11} + \rho_{22} + \rho_{33} + \rho_{44} = 1$ .

To investigate the optical response of the probe field, we solve for the density matrix element  $\rho_{41}$  associated with the probe transition under the steady-state condition. From Eqs. (7), (8) and (9), the solution is obtained, within the weak-probe approximation, as:

$$\rho_{41} = \frac{\frac{i}{2}\Omega_p}{\gamma_{41} - i(\Delta_p + \Delta_B) + \frac{(\Omega_s/2)^2}{\gamma_{42} - i(\Delta_p - \Delta_s + 2\Delta_B)} + \frac{(\Omega_c/2)^2}{\gamma_{43} - i(\Delta_p - \Delta_c + \Delta_B)}}. \quad (13)$$

This matrix element is directly related to the complex susceptibility  $\chi_p$  of the probe laser field for the  $|1\rangle \leftrightarrow |4\rangle$  transition as:

$$\chi_p = \frac{N|d_{41}|^2}{2\hbar\epsilon_0\Omega_p}\rho_{41}, \quad (14)$$

where  $N$  is the electron number density and  $\epsilon_0$  is permittivity in free space, respectively. As a result, the absorption and dispersion coefficients for the probe laser field are directly proportional

to the imaginary and real components  $\text{Im}(\rho_{41})$  and  $\text{Re}(\rho_{41})$ , respectively. Subsequently, the group index is related to the dispersion through the following relation:

$$n_g(\omega_p) = \frac{1}{2}\text{Re}(\chi_p) + \frac{\omega_p}{2} \frac{\partial \text{Re}(\chi_p)}{\partial \omega_p}. \quad (15)$$

### 3. Results and discussion

To illustrate this configuration, we apply the model to the  $^{87}\text{Rb}$  atomic system with the selected states as follows:

$$\begin{aligned} |1\rangle &= 5S_{1/2}(F = 1, m_F = -1), \\ |2\rangle &= 5S_{1/2}(F = 1, m_F = +1), \\ |3\rangle &= 5S_{1/2}(F = 2, m_F = 0), \\ |4\rangle &= 5P_{3/2}(F' = 2, m_F = 0). \end{aligned}$$

The optical properties of interest in this work include EIT absorption, EIT dispersion, and the group index. For simplicity in simulating the survey results, the frequency-related quantities are normalized by  $\gamma$  of the order of MHz, while the magnetic field strength is normalized by  $\gamma_c = \hbar g_F^{-1} \mu_B^{-1} \gamma$ .

First, we investigate the influence of the magnetic field on the EIT spectrum by fixing the parameters of the laser fields at  $\Omega_c = \Omega_s = 5\gamma$  and  $\Delta_c = \Delta_s = 0$  and plotting the absorption both in the absence ( $B = 0$ ) and in the presence ( $B = \pm 5\gamma_c$ ) of the external magnetic field, as shown in Fig. 2. In principle, this four-level configuration can give rise to two EIT windows induced by the coupling field  $\Omega_c$  and the signal field  $\Omega_s$  which satisfy the two-photon resonance conditions  $\Delta_p + \Delta_B - \Delta_c = 0$  and  $\Delta_p + 2\Delta_B - \Delta_s = 0$ , respectively. Therefore, if we choose  $\Delta_c = \Delta_s = 0$ , the EIT windows will be located at the positions  $\Delta_p = -\Delta_B$  (induced by  $\Omega_c$ ) and  $\Delta_p = -2\Delta_B$  (induced by  $\Omega_s$ ), respectively (see Fig. 1). Thus, when  $B = 0$  (Fig. 2a), the degenerate energy levels  $|1\rangle$  and  $|2\rangle$  overlap, while the control lasers are chosen to be on resonance ( $\Delta_c = \Delta_s = 0$ ). As a result, the two EIT windows also overlap at the probe resonance position  $\Delta_p = 0$ . On the other hand, when the magnetic field with strength  $B = \pm 5\gamma_c$  is applied, the levels  $|1\rangle$  and  $|2\rangle$  are split by the Zeeman effect by an amount  $\Delta_B$  proportional to the field strength  $B$ . This shift in energy levels leads to the displacement of the EIT windows, resulting in two separate transparency windows. For instance, when  $B = 5\gamma_c$ , the EIT window induced by the coupling field is shifted to  $\Delta_p = -\Delta_B = -5\gamma$  that satisfying the two-photon resonance condition  $\Delta_p + \Delta_B - \Delta_c = 0$ . Meanwhile, the EIT window induced by the signal field is shifted to  $\Delta_p = -2\Delta_B = -10\gamma$  that satisfying the two-photon resonance condition  $\Delta_p + 2\Delta_B - \Delta_s = 0$ , as represented by the dashed line in Fig. 2(b). Similarly, when  $B = -5\gamma_c$ , the two EIT windows appear at  $\Delta_p = -\Delta_B = 5\gamma$  and  $\Delta_p = -2\Delta_B = 10\gamma$ , respectively (see the solid line in Fig. 2b). Furthermore, we also notice that the shift in the EIT windows modifies the absorption at the probe resonance. For example, while the probe is transparent at resonance when  $B = 0$ , it undergoes strong absorption when  $B \neq 0$ .

We also note that, compared with the model in Ref. [20], which exhibits a single EIT window for each probe polarization but allows flexible switching of the optical response between the polarization components, the present model can generate two EIT windows for a chosen probe polarization and allows switching between transparency and absorption regimes.

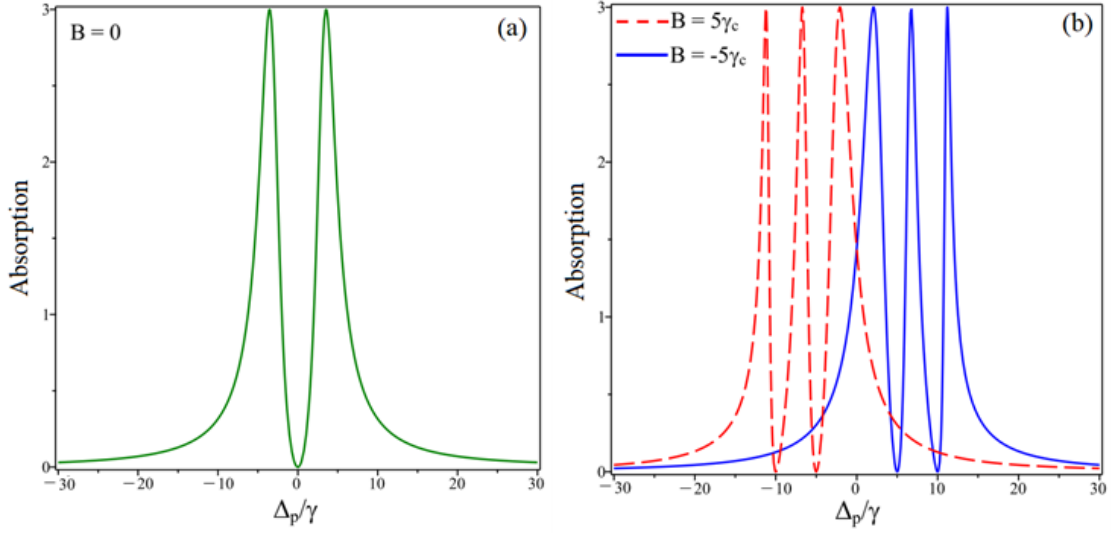


**Fig. 2.** EIT spectrum of the probe beam for  $B = 0$  (a) and  $B = \pm 5\gamma_c$  (b). The control beam parameters are  $\Omega_c = \Omega_s = 5\gamma$  and  $\Delta_c = \Delta_s = 0$ .

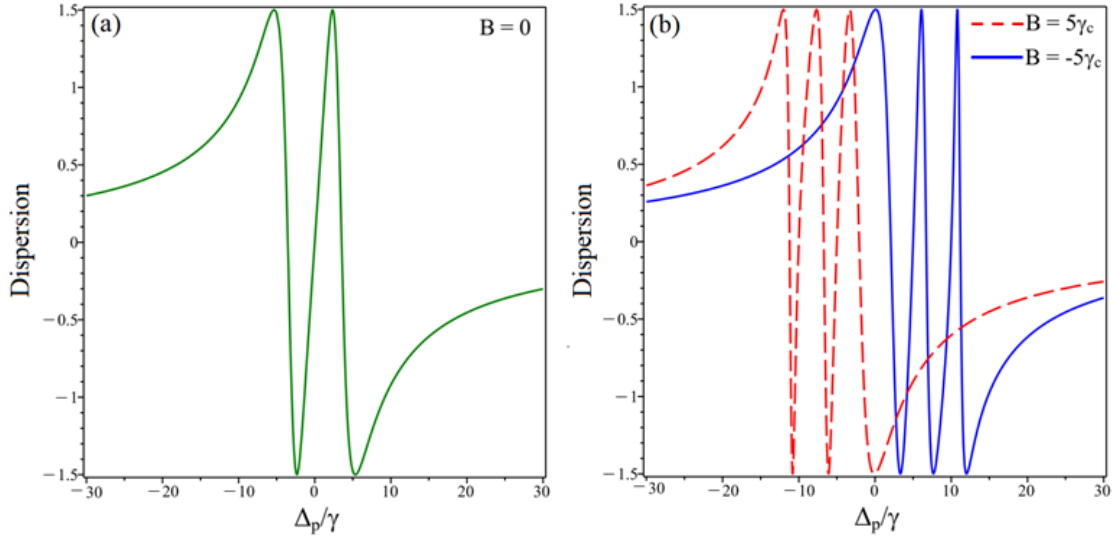


**Fig. 3.** EIT dispersion of the probe beam for  $B = 0$  (a) and  $B = \pm 5\gamma_c$  (b). The control beam parameters are  $\Omega_c = \Omega_s = 5\gamma$  and  $\Delta_c = \Delta_s = 0$ .

The changes in absorption lead to corresponding changes in dispersion, following the Kramers-Kronig relation, as illustrated in Fig. 3. Here, the dispersion curves are plotted in the same manner as the absorption spectra in Fig. 2. From Fig. 3, it is clear that a normal dispersion curve appears at the position of the EIT window when  $B = 0$  (Fig. 3a), whereas two such dispersion curves emerge at the two EIT windows when  $B \neq 0$ , as shown in Fig. 3(b). The anomalous

dispersion curves, in turn, are located alternately between the normal dispersion curves. Thus, the magnetic-field-induced shift of the dispersion curves also modifies the dispersion properties in the probe resonance region; specifically, the system exhibits normal dispersion when  $B = 0$ , while anomalous dispersion arises when  $B \neq 0$ .

To better illustrate the changes in absorption and dispersion in the presence of a magnetic field, we fix the probe laser frequency at resonance ( $\Delta_p = 0$ ) and plot the absorption and dispersion as functions of the magnetic field, as shown in Fig. 4. The dashed line shows that, at resonance, the probe absorption is nearly zero when  $B = 0$ , increases gradually with increasing magnetic field strength, and then decreases in the off-resonant region. Similarly, the dispersion curve also increases in the resonance region as the magnetic field grows but then decreases and even changes sign in the off-resonant region when the magnetic field continues to increase.

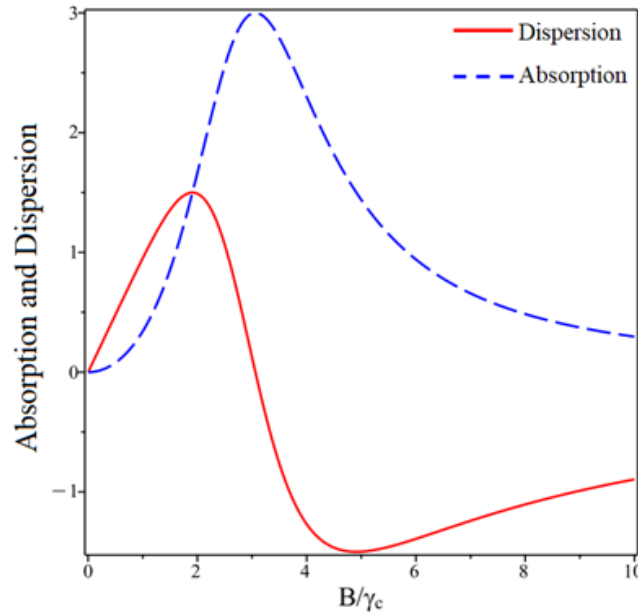


**Fig. 4.** Variations of probe absorption (dashed line) and dispersion (solid line) as a function of magnetic field strength. The control beam parameters are  $\Omega_c = \Omega_s = 5\gamma$  and  $\Delta_p = \Delta_c = \Delta_s = 0$ .

Next, we examine the influence of the magnetic field on the group index under EIT conditions. The group index is a parameter that determines the propagation of a light pulse in the medium, either in the slow-light or fast-light regime. A positive group index (corresponding to normal dispersion) gives rise to slow light, while a negative group index (corresponding to anomalous dispersion) leads to fast light propagation. The magnitude of the group index depends on both the slope and the amplitude of the dispersion curve.

In Fig. 5, we plot the group index with the same parameters as in Fig. 2. Fig. 5(a) corresponds to  $B = 0$  (no external magnetic field) with the laser parameters set to  $\Omega_c = \Omega_s = 5\gamma$  and  $\Delta_p = \Delta_c = \Delta_s = 0$ . In this case, only one EIT window appears at the probe resonance center  $\Delta_p = 0$ ,

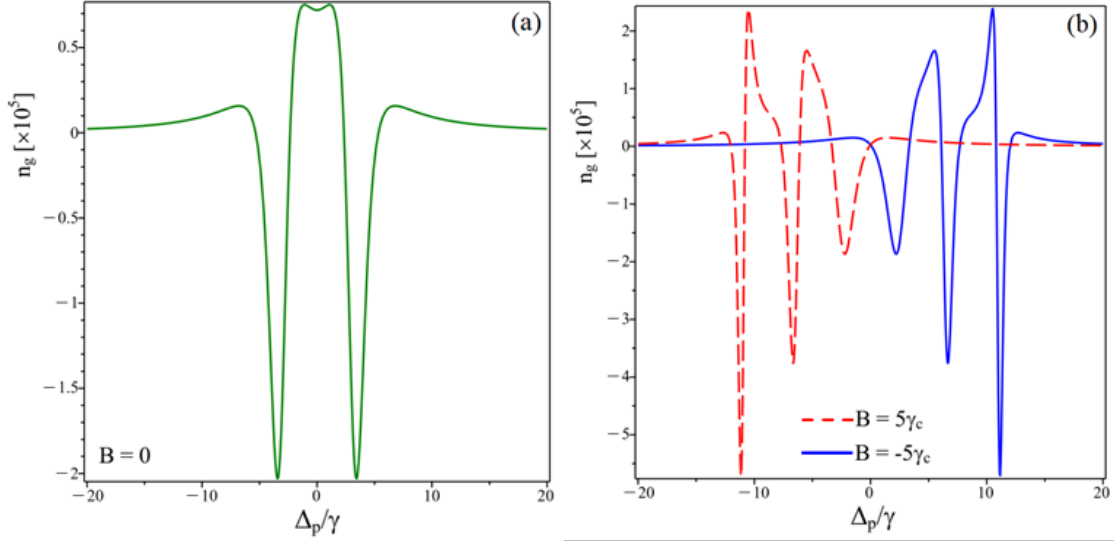


**Fig. 5.** Group index for the probe beam when  $B = 0$  (a) and  $B = \pm 5\gamma_c$  (b). The control beam parameters are  $\Omega_c = \Omega_s = 5\gamma$  and  $\Delta_c = \Delta_s = 0$ .

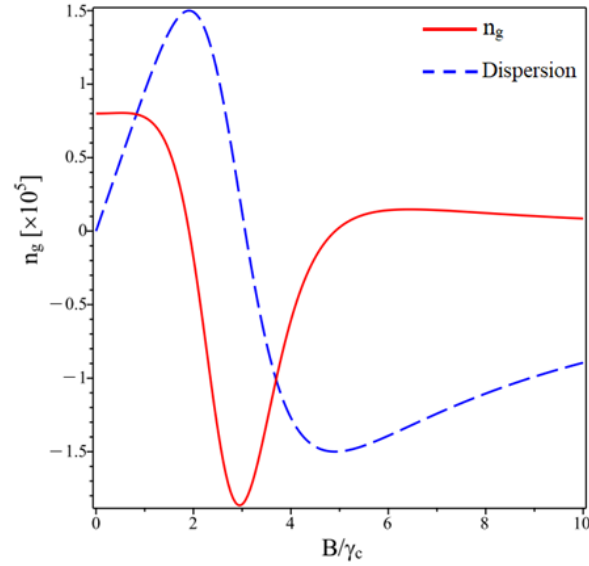


**Fig. 6.** Variations of group index (solid line) and dispersion (dashed line) as a function of magnetic field strength. The control beam parameters are  $\Omega_c = \Omega_s = 5\gamma$  and  $\Delta_p = \Delta_c = \Delta_s = 0$ .

giving rise to normal dispersion and hence a positive group index. We also find that the group index amplitude is quite large, on the order of  $10^5$ , which leads to the propagation of ultraslow light pulses. Outside the resonance region, anomalous dispersion dominates, resulting in a negative

group index and thus fast-light propagation. Fig. 5(b) corresponds to  $B = \pm 5\gamma_c$ , where, as shown previously, two separate EIT windows appear. For  $B = 5\gamma_c$  (dashed line), the two EIT windows are located at probe frequency positions  $\Delta_p = -5\gamma$  and  $\Delta_p = -10\gamma$ . These regions correspond to positive group indices (slow light), interleaved with regions of negative group indices (fast light). Similarly, when  $B = -5\gamma_c$ , the positive group-index regions are located at  $\Delta_p = 5\gamma$  and  $\Delta_p = 10\gamma$ , alternating with negative group-index regions.

Finally, in Fig. 6 we investigate the variation of the group index (solid line) and dispersion (dashed line) as functions of the external magnetic field at the probe resonance frequency  $\Delta_p = 0$ . The results show that both the magnitude and the sign of the group index vary with the magnetic field strength. This behavior of the group index is consistent with the corresponding changes in the amplitude and sign of the dispersion curve (dashed line). That is, an increase in normal dispersion leads to an increase in the positive group index, whereas an increase in anomalous dispersion results in an increase in the negative group index.

#### 4. Conclusion

We have developed an analytical model to investigate the optical response of a degenerate four-level  $\Lambda$ -type atomic system under an external magnetic field. Our results show that by tuning the magnetic field, the system can be switched between single- and double-EIT regimes, enabling flexible control of absorption, dispersion, and group index. For example, at  $B = 0$ , the system exhibits a single EIT window at resonance ( $\Delta_p = 0$ ), whereas at  $B = +5\gamma$ , the two EIT windows are separated and located at  $\Delta_p = -5\gamma$  and  $\Delta_p = -10\gamma$ ; a similar behavior occurs for  $B = -5\gamma$ . Such shifts and splitting of the EIT positions lead to corresponding changes in the dispersion and group index curves, allowing the selection of desired frequency regions for different response regimes.

Compared with Ref. [20], which used a single control field and a probe with left- and right-circular polarization components in a ladder-type configuration, the present work employs a  $\Lambda$ -type configuration with two independent control fields, enabling two distinct and tunable EIT windows. This scheme allows flexible switching between single- and double-EIT regimes and provides stronger ground-state coherence and higher transparency efficiency, making it more suitable for experimental implementation and applications. These findings offer valuable insights for potential applications in optical switching, light storage, and quantum information technologies.

#### Acknowledgments

This research was funded by Vingroup Innovation Foundation (VINIF) under project code VINIF.2022.DA00076.

#### Conflict of interest

The authors declare no competing interests.

#### References

- [1] K. J. Boller, A. Imamoglu and S. E. Harris, *Observation of electromagnetically induced transparency*, [Phys. Rev. Lett.](#) **66** (1991) 2593.
- [2] M. Fleischhauer, A. Imamoglu and J. P. Marangos, *Electromagnetically induced transparency: Optics in coherent media*, [Rev. Mod. Phys.](#) **77** (2005) 633.

- [3] N. H. Bang, L. V. Doai and D. X. Khoa, *Controllable optical properties of multi-electromagnetically induced transparency in gaseous atomic medium*, *Comm. Phys.* **29** (2019) 1.
- [4] D. McGloin, D. J. Fullton and M. H. Dunn, *Electromagnetically induced transparency in n-level cascade schemes*, *Opt. Commun.* **190** (2001) 221.
- [5] L. V. Hau, S. E. Harris, Z. Dutton and C. H. Bejroozi, *Light speed reduction to 17 metres per second in an ultracold atomic gas*, *Nature* **397** (1999) 594.
- [6] N. H. Bang, N. V. Ai, D. H. Son, P. V. Thuan, L. T. Y. Nga, H. H. Quang *et al.*, *Observation of giant group index in a multi-level  $^{85}\text{Rb}$  atomic medium at room temperature*, *Opt. Lett.* **49** (2024) 4787.
- [7] H. Kang and Y. Zhu, *Observation of large kerr nonlinearity at low light intensities*, *Phys. Rev. Lett.* **91** (2003) 093601.
- [8] L. T. Y. Nga, N. H. Bang, N. V. Phu, H. M. Dong, N. T. T. Hien, N. V. Ai *et al.*, *Variable kerr nonlinearity and optical bistability of a four-level lambda atomic medium*, *Chaos Solitons Fractals* **191** (2025) 115870.
- [9] M. Sahraei, S. H. Asadpour, H. Mahrami and R. Sadighi-Bonabi, *Controlling the optical bistability via quantum interference in a four-level n-type atomic system*, *J. Lumin.* **131** (2011) 1682.
- [10] D. X. Khoa, L. V. Doai, L. N. M. Anh, L. C. Trung, P. V. Thuan, N. T. Dung *et al.*, *Optical bistability in a five-level cascade atomic medium: An analytical approach*, *J. Opt. Soc. Am. B* **33** (2016) 735.
- [11] D. X. Khoa, N. V. Ai, H. M. Dong, L. V. Doai and N. H. Bang, *All-optical switching in a medium of a four-level vee-cascade atomic medium*, *Opt. Quantum Electron.* **54** (2022) 164.
- [12] L.-G. Si, X.-Y. Lu, X. Hao and J.-H. Li, *Dynamical control of soliton formation and propagation in a y-type atomic system with dual ladder-type electromagnetically induced transparency*, *J. Phys. B* **43** (2010) 065403.
- [13] H. M. Dong, N. T. T. Hien, N. H. Bang and L. V. Doai, *Dynamics of twin pulse propagation and dual-optical switching in a  $\lambda + \xi$  atomic medium*, *Chaos Solitons Fractals* **178** (2024) 114304.
- [14] K. Cox, V. I. Yudin, A. V. Taichenachev, I. Novikova and E. E. Mikhailov, *Measurements of the magnetic field vector using multiple electromagnetically induced transparency resonances in Rb vapor*, *Phys. Rev. A* **83** (2011) 015801.
- [15] P. Kaur and A. Wasan, *Effect of magnetic field on the optical properties of an inhomogeneously broadened multi-level  $\lambda$ -system in Rb vapor*, *Eur. Phys. J. D* **71** (2017) 78.
- [16] C. Mishra, A. Chakraborty, A. Srivastava, S. K. Tiwari, S. P. Ram, V. B. Tiwari *et al.*, *Electromagnetically induced transparency in  $\lambda$ -systems of  $^{87}\text{Rb}$  atom in magnetic field*, *J. Mod. Opt.* **65** (2018) 2269.
- [17] N. H. Bang and L. V. Doai, *Modifying optical properties of three-level v-type atomic medium by varying external magnetic field*, *Phys. Scr.* **95** (2020) 105103.
- [18] S. H. Asadpour, H. R. Hamed and H. R. Soleimani, *Slow light propagation and bistable switching in a graphene under an external magnetic field*, *Laser Phys. Lett.* **12** (2015) 045202.
- [19] H. M. Dong, T. D. Thanh, N. H. Bang and L. V. Doai, *Static magnetic field swaps slow and fast light in a v-type degenerate media*, *IEEE Photonics Technol. Lett.* **37** (2025) 813.
- [20] N. V. Phu, N. H. Bang, L. T. Y. Nga and L. V. Doai, *Switching between slow light and fast light by static magnetic field in a degenerate four-level atomic system at room temperature*, *J. Opt.* **26** (2024) 065403.
- [21] N. H. Bang, D. X. Khoa and L. V. Doai, *Controlling self-kerr nonlinearity with an external magnetic field in a degenerate two-level inhomogeneously broadened medium*, *Phys. Lett. A* **384** (2020) 126234.
- [22] N. T. T. Hien, N. L. Dan, N. H. Bang, D. X. Khoa, N. V. Phu, N. T. L. Anh *et al.*, *Two-channel optical bistability and multistability in a degenerate four-level atomic medium under a static magnetic field*, *Sci. Rep.* **14** (2024) 19007.
- [23] H. M. Dong, D. X. Khoa, L. V. Doai, N. V. Tam and L. T. Y. Nga, *High-efficiency two-channel magneto-optical switching and kerr nonlinearity control using a static magnetic field in a degenerate four-level atomic medium*, *J. Opt. Soc. Am. B* **42** (2025) 1601.
- [24] R. Yu, J. Li, C. Ding and X. Yang, *Dual-channel all-optical switching with tunable frequency in a five-level double-ladder atomic system*, *Opt. Commun.* **284** (2011) 2930.
- [25] J. Li, R. Yu, L. Si and X. Yang, *Propagation of twin light pulses under magneto-optical switching operations in a four-level inverted-y atomic medium*, *J. Phys. B* **43** (2010) 065502.